DNA Repair 10 (2011) 1044–1050

Contents lists available at ScienceDirect

DNA Repair

journal homepage: www.elsevier.com/locate/dnarepair

Involvement of *MRE11A* and *XPA* gene polymorphisms in the modulation of DNA double-strand break repair activity: A genotype–phenotype correlation study

Fulvio Ricceri[a,b,1], Paola Porcedda[c,d,1], Alessandra Allione[a,1], Valentina Turinetto[c], Silvia Polidoro[a], Simonetta Guarrera[a], Fabio Rosa[a], Floriana Voglino[a], Annamaria Pezzotti[a], Valentina Minieri[c], Lisa Accomasso[c], Elisa Cibrario Rocchietti[c], Luca Orlando[c], Claudia Giachino[c], Giuseppe Matullo[a,b,*]

[a] *Human Genetics Foundation – HuGeF, Turin, Italy*
[b] *Department of Genetics, Biology and Biochemistry, University of Turin, Turin, Italy*
[c] *Department of Clinical and Biological Sciences, University of Turin, Turin, Italy*
[d] *Department of Thermodynamics, Istituto Nazionale di Ricerca Metrologica – INRiM, Turin, Italy*

ARTICLE INFO

Article history:
Received 20 May 2011
Received in revised form 25 July 2011
Accepted 7 August 2011
Available online 30 August 2011

Keywords:
DNA repair
Double-strand break repair
MRE11A
XPA
H2AX phosphorylation

ABSTRACT

DNA double-strand breaks (DSB) are the most lethal form of ionizing radiation-induced DNA damage, and failure to repair them results in cell death. In order to see if any associations exist between DNA repair gene polymorphisms and phenotypic profiles of DSB repair (DSBR) we performed a genotype–phenotype correlation study in 118 young healthy subjects (mean age 25.8 ± 6.7 years). Subjects were genotyped for 768 single nucleotide polymorphisms (SNPs) with a custom Illumina Golden Gate Assay, and an H2AX histone phosphorylation assay was done to test DSBR capacity.

We found that H2AX phosphorylation at 1 h was significantly lower in subjects heterozygous (no variant homozygotes were observed) for the *XPA* gene SNP rs3176683 (p-value = 0.005), while dephosphorylation was significantly higher in subjects carrying the variant allele in three *MRE11A* gene SNPs: rs1014666, rs476137 and rs2508784 (p-value = 0.003, 0.003 and 0.008, respectively). An additive effect of low-activity DNA repair alleles was associated with altered DSBR activity, as demonstrated by both H2AX phosphorylation at 1 h (p-trend <0.0001) and γH2AX dephosphorylation at 3 h (p-trend <0.0001).

Our study revealed that in addition to SNPs of genes that are well-established players in DSBR, non-DSBR genes, such as the *XPA* gene that is mainly involved in the nucleotide excision repair pathway, can also influence DSBR in healthy subjects. This suggests that successful DSBR may require both DSBR and non-DSBR mechanisms.

1. Introduction

Cellular DNA can suffer from a wide range of damage, both from extra-cellular agents (ionizing radiation, UV light and environmental chemicals) and *via* endogenous mechanisms (depurination, deamination and mistakes in double-strand replication or recombination).

DNA damage is repaired through five different pathways: base excision repair (BER), nucleotide excision repair (NER), mismatch repair (MMR), double-strand break repair (DSBR) and direct repair (DR). BER is mainly involved in the correction of non-bulky damage, while NER is involved in the correction of lesions that disrupt the double-helical structure of DNA. Replication errors are corrected through MMR; DSBs are repaired through two different DSBR pathways: homologous and non-homologous recombination; and finally correction of methylated or alkylated bases occurs through DR [1].

At the end of last century the relevance of DNA repair mechanisms in human carcinogenesis was assessed [2] and phenotypic variations related to cancer risk have increased exponentially in recent years. Indeed, genetic variation in some of the DNA repair genes involved in the five pathways mentioned above appears to influence an individual's susceptibility to cancer [3–5]. However, in most cases no clear genotype–phenotype relationship has been found.

Abbreviations: SNP, single nucleotide polymorphism; PBMC, peripheral blood mononuclear cells; DSB, double-strand break; DSBR, double-strand break repair; IR, ionizing radiation; NER, nucleotide excision repair; LD, linkage disequilibrium; MRN complex, MRE11–RAD50–NBS1 complex; ICL, inter-strand crosslinks; MAF, minor allele frequency.

* Corresponding author at: Department of Genetics, Biology and Biochemistry, University of Turin, Via Santena 19, I-10126 Turin, Italy. Tel.: +39 0116708450; fax: +39 0112365601.
E-mail address: giuseppe.matullo@unito.it (G. Matullo).
[1] Equally contributed.

1568-7864/$ – see front matter © 2011 Elsevier B.V. All rights reserved.
doi:10.1016/j.dnarep.2011.08.003

Double-strand breaks (DSB) are the most lethal form of ionizing radiation-induced DNA damage. Failure to repair these breaks results in cell death. Immediately following cellular exposure to ionizing radiation, resulting damage is detected by the MRE11/RAD50/NBS1 complex (MRN complex), resulting in rapid recruitment of signaling and repair proteins and alteration of chromatin structure, including histone modifications, to permit proteins to access DNA [6]. MRE11/RAD50 tethers broken DNA ends and NBS1 recruits ATM [7]. Upon activation, ATM phosphorylates the histone H2AX, thus promoting DSBR and amplifying DSB signaling [8], as well as promoting p53, NBS1, CHK2, and other proteins to activate cell cycle checkpoints [7].

Recent studies have shown increasing evidence that these different DNA repair pathways are not independent, but are instead strictly linked. In addition, it has been suggested that non-DSB DNA repair pathways, such as NER and MMR, play an active role in DSBR [9]. The goal of the present study was to see what associations might exist between DNA repair gene polymorphisms and phenotypic profiles of DSBR. This study could thus either reveal novel cross-talks and interplays between different DNA repair pathways, or reinforce previous findings.

2. Materials and methods

2.1. Study population

One hundred eighteen young healthy subjects aged 19–48 years (39 males, 79 females; mean age 25.8 years, median age 23.4 years) were included in the present study. Subjects were mainly recruited at the University of Turin (North-Western Italy). Information on lifestyle habits (diet, smoking and alcohol consumption), prescription drugs and other exposures was collected through self-administered questionnaires. This ethnically homogenous cohort included only Caucasian subjects and was restricted to subjects aged 19–48 years. It is therefore suitable for the investigation of the relationship between DNA repair gene polymorphisms and DNA repair rates as assessed by *in vitro* functional assays.

2.2. Lymphocyte isolation

Thirty ml of heparinized venous blood were collected from all subjects. Peripheral blood mononuclear cells (PBMCs) were separated by centrifugation with Ficoll Paque PLUS (GE Healthcare, Milan, Italy) at $400 \times g$ for 30 min at room temperature. After two washes in RPMI 1640 (Invitrogen, Paisley, UK), 1% FBS (Invitrogen), 25 mM EDTA (Invitrogen), PBMCs were prepared for cryopreservation. They were resuspended at 10×10^6 cells/ml in freezing medium (RPMI 1640, 50% FBS, 10% DMSO), aliquoted in cryovials and slowly frozen overnight at the rate of $-1\,^{\circ}C$/min in isopropyl alcohol to $-80\,^{\circ}C$ (Mr. Frosty containers, Nalgene, Roskilde, Denmark). Cryovials were then transferred into liquid nitrogen for long-term storage.

2.3. DNA extraction

DNA was purified from whole blood cells by the commercial QIAamp DNA Mini Kit silica-membrane-based spin-columns (Qiagen Spa, Milan, Italy) according to the manufacturer's instructions.

2.4. SNP selection for Illumina Golden Gate chip

We selected 62 out of 150 DNA repair genes belonging to the five main DNA repair pathways (see Supplementary Materials and Methods for details). The DNA repair gene SNPs were selected using the list provided by Wood et al. as a guide [10,11]. The SNP selection strategies were as follows.

(i) Tag SNP selection: HapMap genotype data for the Caucasian population (CEU – Release23A, March 2008) were used to select tag SNPs for each of the 62 genes included. Five kb upstream and 1 kb downstream of the gene coordinate were included in the selection. Only SNPs showing a minor allele frequency (MAF) of 0.05 or greater were included for the identification of haplotype blocks using Haploview 4.1 (http://www.broad.mit.edu/mpg/haploview/). A pairwise tagging method with an R^2 threshold of 0.8 was used to run the "Tagger" option in the Haploview 4.1 package, leading to the identification of 524 linkage disequilibrium (LD) blocks, grouping a total of 2053 SNPs.

(ii) "Functional" SNPs selection: "functional" SNPs were defined as those that were predicted by *in silico* methods to have a putative effect on the phenotype, i.e., that cause an amino acid change, those that may alter the functional or structural properties of the translated protein, disrupt transcription factor binding sites, disrupt splice sites or other functional sites (see Supplementary Materials and Methods for details). The selection included 165 SNPs with a possible deleterious effect.

The final list of SNPs after selection, filter and redundancy applications were applied (see Supplementary Materials and Methods) included 768 SNPs (Supplementary Table I). Seventy of these failed to pass the quality control filter (Supplementary Table I) either because they had a call rate below 95%, or because Golden Gate genotyping failed.

Therefore, a total of 698 SNPs were included in the final statistical analyses. Seven SNPs showed deviation from the Hardy–Weinberg equilibrium, but none of them was found to be significantly associated with a phenotype.

2.5. The Golden Gate chip

The Illumina Golden Gate Assay (Universal-32 BeadChip 768 Bead Types V7a, Illumina, Inc., San Diego, CA, USA) was performed according to the manufacturer's instructions (ref. GoldenGate_Genotyping_Assay_Guide_15004065_B). A universal 32-bead chip was used, allowing the simultaneous analysis of 32 samples. An iScan System was used for chip scan and image acquisition, and data analysis was performed with the dedicated Genome Studio v.2009.1 software (Illumina, Inc.).

2.6. H2AX phosphorylation assay

PBMCs were thawed and allowed to recover overnight in complete RPMI 1640 (Invitrogen) supplemented with 10% fetal calf serum (heat inactivated at 56 °C for 30 min) (Invitrogen). Cells were γ-irradiated (2 Gy) using a 6 MV accelerator (Elekta, Stockholm, Sweden) at 2 Gy/min. They were kept on ice for 1 h (the time needed to reach the laboratories), and then returned to the incubator and harvested at 1 h and 3 h. Cells were stained with anti-phospho-histone H2AX (Ser-139) (Upstate Biotechnology, Charlottesville, VA, USA) according to Olive et al. [12,13], with minor modifications [14].

Approximately 400,000 irradiated cells were collected, fixed in cold 70% ethanol and stored at −20 °C for up to 2 weeks before analysis. Cells were washed in Tris-buffered saline pH 7.4 (TBS) and then rehydrated for 10 min at 4 °C in TBS containing 4% FBS and 0.1% Triton X-100 (TST) (Sigma–Aldrich Co., St. Louis, MO, USA) prior to staining with anti-γH2AX mAb (Upstate Biotechnology) diluted at 1:250 in TST, and incubated for 2 h at 37 °C. After two washes in TBS, they were resuspended in FITC-conjugated goat anti-mouse IgG1 (BD PharMingen, Becton Dickinson & Co., Franklin Lakes, NJ, USA) diluted at 1:50 in TST as a secondary antibody, and shaken for 1 h at room temperature in the dark. A minimum of 10,000 stained cells were acquired on a FACScan (Becton Dickinson & Co.) and analyzed with the CellQuest software. We maintained the same cytometer setting for staining on different days (SSC: voltage 402, AmpGain 1, Mode lin., FL1: voltage 490, AmpGain 1, Mode log). In order to normalize the results, aliquots of PBMCs derived from the same subject were used at each irradiation and staining step as control.

The data corresponding to the amount of H2AX phosphorylation at 1 h are expressed as ratio of the median of fluorescence of γH2AX in the sample, relative to the median of fluorescence expressed by the control. The data corresponding to the residual phosphorylation of H2AX after 3 h of recovery are expressed as percentage of the median of γH2AX fluorescence at 3 h with respect to the median of γH2AX fluorescence shown at 1 h by the same sample.

2.7. Haplotype reconstruction

To identify haplotypes, we considered different blocks, one for each gene, with the exception of genes in which there were more than 15 SNPs, for which we divided the genes in different blocks according to their LD pattern. In each block we phased the haplotype using a Bayesian method in which the *a priori* was based on an approximation to the coalescent and the inference was based on the Markov Chain Monte Carlo approach. The LD analysis was performed with Haploview 4.1 [15]; the phase of the haplotypes was inferred using PHASE 2.1 [16,17]. Haplotypes with a frequency lower than 4% were analyzed together as "rare" haplotypes. Haplotype analysis was performed by comparing the Kruskal–Wallis test in subjects with 1 or 2 copies of a specific haplotype to subjects with no copies of that haplotype.

2.8. Statistical analysis

Differences among categories were tested using a two-sided Wilcoxon Rank Sum test or a Kruskal–Wallis test, in the cases of 2 and 3 independent groups, respectively.

The sum of low-activity alleles was computed for each subject by adding the number of alleles that have a putative effect on DSBR capacity (resulting from SNP analyses). We tested the relationship between DSBR capacity and allele score by a linear regression model (p for trend).

For the descriptive and haplotype analyses, a p-value lower than 0.05 was considered significant. For the Golden Gate analyses, considering multiple comparisons and the *a priori* hypotheses for these genotypes, the α level was set at 0.005.

Table 1
Mean values of H2AX phosphorylation at 1 h and γH2AX dephosphorylation at 3 h in relation to sex, age and smoking status among healthy subjects.

Variable	Number of subjects	H2AX phosphorylation at 1 h mean (SD)	*p*-Value[a]	γH2AX dephosphorylation at 3 h mean (SD)	*p*-Value [a]
Sex					
Male	39	0.95 (0.17)	0.04	15.96 (9.93)	0.08
Female	79	0.88 (0.14)		20.21 (11.11)	
Age					
<30	90	0.91 (0.16)	0.16	18.74 (10.05)	0.57
≥30	28	0.86 (0.14)		19.02 (13.40)	
Smoking status					
Never	85	0.89 (0.15)	0.54	19.44 (11.26)	0.34
Ever	32	0.92 (0.16)		16.38 (8.80)	

[a] *p*-Values from the Wilcoxon Rank Sum test.

3. Results

3.1. DNA repair gene SNPs and H2AX phosphorylation and γH2AX dephosphorylation

In Table 1, we present the mean values of H2AX phosphorylation at 1 h, and of γH2AX dephosphorylation at 3 h in relation to sex, age and smoking status. No significant difference was observed between age groups of above/below 30 years old, or for smoking status. A statistically significant difference (p-value = 0.04) was shown for H2AX phosphorylation at 1 h between males (mean ± SD, 0.95 ± 0.17) and females (0.88 ± 0.14), whereas γH2AX dephosphorylation at 3 h did not reach the level of significance (p-value = 0.08) in the gender comparison (Table 1).

Tables 2 and 3 show the SNPs with the highest level of significance (p-value <0.02) for H2AX phosphorylation at 1 h and γH2AX dephosphorylation at 3 h, respectively. Phosphorylation at 1 h was significantly lower (p-value = 0.005) in subjects heterozygous for the *XPA* gene SNP rs3176683 (no variant homozygotes were observed). γH2AX dephosphorylation was significantly higher (with an increasing trend) in subjects carrying the variant allele in three different *MRE11A* gene SNPs: rs1014666, rs476137, rs2508784 (p-value = 0.003, 0.003, 0.008, respectively). SNPs rs1014666 and rs2508784 are in strong LD (R^2 = 0.97, 1000 Genomes database), though they have a lower LD with respect to rs476137 (R^2 = 0.78 and R^2 = 0.74, respectively). All the other SNPs associated with DSBR capacity listed in Tables 2 and 3 had p-values between 0.01 and 0.02.

3.2. Haplotype analysis

XPA and *MRE11A* gene haplotype analyses confirmed the results obtained in single SNP analyses (Tables 4 and 5). The *XPA* gene haplotype ID #2 (AGGGAAGG) was related to a higher proportion of H2AX phosphorylation at 1 h (p-value = 0.038) in the presence of one or two copies (0.95 ± 0.16 and 0.90 ± 0.13, respectively) versus 0 copies (0.70 ± 0.15) (Table 4). Even the *XPA* gene haplotype ID #8 (GGGGAGGC) was significantly associated (p-value = 0.005) with higher H2AX phosphorylation at 1 h for subjects carrying 1 copy of the haplotype (1.00 ± 0.16 versus 0.88 ± 0.15 with 0 copies), whereas haplotype ID #9 (GGGGAAAG) was associated (p-value = 0.004) with decreased H2AX phosphorylation at 1 h (Table 4).

The *MRE11A* gene haplotype analyses (Table 5) suggested an increased γH2AX dephosphorylation at 3 h for haplotype ID #10 (GGAAACAA) (p-value = 0.025; 19.64 ± 10.27, 19.94 ± 12.03 and 11.11 ± 6.75 for 0, 1 and 2 copies, respectively) and for all rare haplotypes combined (p-value = 0.01; 19.64 ± 11.03 and 11.45 ± 5.59 for 0 and 1 copies, respectively). On the other hand, *MRE11A* gene haplotype ID #6 (AGAGGAAA) showed decreased γH2AX dephosphorylation at 3 h (p-value = 0.032; 17.71 ± 10.95, 21.17 ± 9.88 and 30.68 ± 9.48 for 0, 1 and 2 copies, respectively).

3.3. DSBR capacity allele score

Fig. 1 shows the relationship between DSBR capacity (A: H2AX phosphorylation at 1 h; B: γH2AX dephosphorylation at 3 h) and the sum of low-activity alleles in DNA repair genes identified in Tables 2 and 3. When defining the SNPs that contribute to modulating DSBR capacity for the purposes of this study, SNPs were selected based on the LD pattern (avoiding redundancy of information from SNPs in strong LD) and on the existence of a plausible genetic transmission model (recessive, dominant and codominant).

An additive effect of low-activity DNA repair alleles was associated with (a) decreased DSB signaling capacity, as calculated from H2AX phosphorylation values at 1 h (p-trend <0.0001) and (b) decreased γH2AX dephosphorylation at 3 h (p-trend <0.0001).

4. Discussion

The aim of our study was to identify a relationship between low-penetrance variants of DNA repair genes and DSBR activity, measured as phosphorylation and dephosphorylation of the H2AX histone following ionizing radiation (IR). Our results showed a strong correlation between the *MRE11A* DNA repair gene (on both a SNP and a haplotype level) and γH2AX dephosphorylation. Due to the central role of the *MRE11A* gene in DSBR, this correlation fits perfectly with an *a priori* hypothesis.

MRE11A interacts with NBS1 and RAD50 to form the MRN complex, which activates the ATM kinase and participates in DNA damage response with other ATM substrates. It can also function to tether broken ends, and may even resect broken ends. Thus, MRE11A plays many fundamental roles in DSB signaling and processing. *MRE11A* gene mutations cause the rare human cancer predisposition disease ataxia telangiectasia-like disorder (ATLD) [18,19]. This disorder clearly establishes the importance of the MRN complex in preventing cancer development and underscores the functional significance of MRE11–ATM interaction. Recent work has suggested that a functional MRN complex may be required for full ATM activation [20], and one study observed that ATM autophosphorylation at Ser-1981 [21], used as a marker for ATM activation, was reduced in the cells of individuals with ATLD and NBS cells, suggesting that a functional MRN complex is also required for autoactivation of ATM. Moreover, another study that used an entirely different system showed ATM activation to be MRE11A-dependent [22].

Only a few *MRE11A* gene SNPs have been associated with an increased risk of tumor development: rs2155209 has been associated with bladder cancer risk [23], and rs601341 with breast cancer [24] and non-Hodgkin lymphoma risk [25]. The *MRE11A* gene

Table 2
Association between individual DNA repair gene SNPs included in the Golden Gate Illumina chip and H2AX phosphorylation at 1 h.

Gene	SNP (rs)	Chrom loc	*p*-Value[a]	H2AX phosphorylation at 1 h			Genotypes			Low-activity alleles (0, 1, 2)[b]
				AA	Aa	aa	AA (n/genotype)	Aa (n/genotype)	aa (n/genotype)	
XPA	3176683	9q22.3	0.005	0.92	0.81		99/AA	19/AG		AA/AG/GG
RAD23B	11573703	9q31.2	0.012	0.87	0.96	0.86	78/AA	38/AG	2/GG	ND
PPP2CB	4733200	8p12	0.014	0.87	0.95	0.80	65/CC	47/CG	6/GG	ND
XPC	3731081	3p25	0.014	0.89	0.89	1.17	70/CC	43/AC	4/AA	AA/AC/CC
XPC	3731124	3p25	0.015	0.89	0.89	1.24	70/AA	45/AC	3/CC	ND
RPA3	3735460	7p22	0.019	0.92	0.83		96/GG	22/AG		GG/AG/AA
PPP2CB	7833839	8p12	0.019	0.88	0.97	0.77	85/GG	30/AG	3/AA	ND
BRCA2	11571789	13q12.3	0.020	0.88	0.98		97/CC	21/AC		AA/AC/CC
XRCC4	3734091	5q14.2	0.022	0.91	0.75		113/CC	5/AC		CC/AC/AA
BRCA2	9567578	13q12.3	0.023	0.89	0.88	1.04	69/AA	40/AG	9/GG	GG/AG/AA
OGG1	293796	3p26.2	0.024	0.90	0.83	1.06	100/GG	14/AG	4/AA	ND
PNKP	2257103	19q13.3–q13.4	0.024	0.95	0.89	0.85	40/GG	51/AG	24/AA	GG/AG/AA

[a] *p*-Values from the Kruskal–Wallis or Wilcoxon Rank Sum test as appropriate; $p \leq 0.02$.
[b] SNPs were coded as low-activity alleles based on data from the γH2AX assay: 0 = homozygous for high-activity allele; 1 = heterozygous, carrying one high- and one low-activity allele; 2 = homozygous for low-activity allele. ND = low-activity allele not evaluable or SNP in linkage disequilibrium with other SNPs in the same table.

Table 3
Association between individual DNA repair gene SNPs included in the Golden Gate Illumina chip and % of γH2AX dephosphorylation at 3 h.

Gene	SNP (rs)	Chrom Loc	*p*-Value[a]	% of γH2AX dephosphorylation at 3 h			Genotypes			Low-activity alleles (0, 1, 2)[b]
				AA	Aa	aa	AA (n/genotype)	Aa (n/genotype)	aa (n/genotype)	
MRE11A	1014666	11q21	0.003	13.13	20.06	21.76	28/AA	63/AG	27/GG	GG/AG/AA
MRE11A	476137	11q21	0.003	13.27	19.78	22.48	27/CC	64/AC	26/AA	ND
MRE11A	2508784	11q21	0.008	13.27	20.05	20.67	27/AA	62/AG	28/GG	ND
MGMT	6482754	10q26	0.010	17.30	24.68		94/GG	24/AG		AA/AG/GG
MRE11A	584531	11q21	0.010	19.64	20.37	10.99	63/AA	39/AG	14/GG	AA/AG/GG
MRE11A	4459257	11q21	0.012	19.64	20.19	10.99	63/AA	41/AG	14/GG	ND
MRE11A	604845	11q21	0.012	19.64	20.21	10.99	64/GG	40/AG	14/AA	ND
RAD23B	11573703	9q31.2	0.012	17.29	22.42	9.30	78/AA	38/AG	2/GG	AA/AG/GG
ATM	654005	11q22-q23	0.015	20.41	15.92	23.68	57/AA	52/AG	8/GG	ND
HTATIP	4244812	11q13	0.016	22.66	18.38	15.00	29/AA	68/AG	20/GG	AA/AG/GG
NHEJ1	2293081	2q35	0.017	19.68	18.16	8.27	89/AA	23/AC	6/CC	AA/AC/CC
MRE11A	541472	11q21	0.019	15.38	20.00	22.72	41/AA	55/AG	21/GG	GG/AG/AA
RPA1	4790838	17p13.3	0.019	15.91	21.41	18.32	47/AA	55/AG	16/GG	ND
ERCC4	1800124	16p13.12	0.020	19.25	8.55		113/AA	5/AG		AA/AG/GG
MGMT	10829618	10q26	0.021	18.23	21.96	5.88	80/CC	33/CG	4/GG	CC/CG/GG
MRE11A	12222920	11q21	0.021	17.54	21.46	30.68	87/CC	28/CG	3/GG	GG/CG/CC

[a] *p*-Values from the Kruskal–Wallis or Wilcoxon Rank Sum test as appropriate; $p \leq 0.02$.
[b] SNPs were coded as low-activity alleles based on data from the γH2AX assay: 0 = homozygous for high-activity allele; 1 = heterozygous, carrying one high- and one low-activity allele; 2 = homozygous for low-activity allele. ND = low-activity allele not evaluable or SNP in linkage disequilibrium with other SNPs in the same table.

Table 4
Association between *XPA* gene haplotypes and H2AX phosphorylation at 1 h.

Haplotype ID	rs2805837	rs2808676	rs2808667	rs2805835	rs3176689	rs3176683	rs3176658	rs10759868	Frequency (*n*)	Frequency (%)
#2	A	G	G	G	A	A	G	G	67	28.4
#3	A	G	G	G	T	A	G	G	36	15.3
#6	G	G	G	G	A	A	G	C	34	14.4
#5	A	A	G	C	A	A	G	G	23	9.7
#4	A	A	G	G	A	A	G	G	21	8.9
#8	G	G	G	G	A	G	G	C	19	8.1
#9	G	G	G	G	A	A	A	G	17	7.2
#11	G	G	A	G	A	A	A	G	15	6.4
#10	G	G	G	G	T	A	G	G	2	0.9
#1	A	G	G	G	A	A	G	C	1	0.4
#7	G	G	G	G	A	A	G	G	1	0.4

Haplotype ID	Number of subjects			H2AX phosphorylation at 1 h mean + SD			*p*-Value[a]
	0 copies	1 copy	2 copies	0 copies	1 copy	2 copies	
#2	62	45	11	0.70 ± 0.15	0.95 ± 0.16	0.90 ± 0.13	0.038
#3	84	32	2	0.91 ± 0.16	0.88 ± 0.13	0.87 ± 0.24	0.722
#6	89	24	5	0.89 ± 0.15	0.95 ± 0.18	0.87 ± 0.09	0.325
#5	95	23	0	0.91 ± 0.15	0.86 ± 0.15		0.156
#4	98	19	1	0.90 ± 0.15	0.91 ± 0.16	0.69 ± 0	0.286
#8	101	17	0	0.88 ± 0.15	1.00 ± 0.16		0.005
#9	99	19	0	0.92 ± 0.15	0.81 ± 0.13		0.004
#11	103	15	0	0.91 ± 0.15	0.84 ± 0.14		0.111
#10, #1, #7	114	4	0	0.90 ± 0.15	0.88 ± 0.11		0.818

[a] *p*-Values from the Kruskal–Wallis or Wilcoxon Rank Sum test as appropriate.

SNPs we identified (rs1014666, rs476137 and rs2508784) are neither non-synonymous, nor in high LD with any non-synonymous SNPs with a known function. However, rs476137 was in LD with rs601341 ($R^2 = 0.80$), one of the SNPs previously associated with cancer risk.

Two isoforms of MRE11A transcripts are expressed: isoform 1, 4772 nt, and isoform 2, 4688 nt, transcribed from an alternative first (non-coding) exon and lacking exon 5 (Atlas of Genetics and Cytogenetics in Oncology and Hematology). Although one of the SNPs we identified, rs1014666, is located at 65 bp from the 5′ terminal of exon 5, the *in silico* prediction (see Supplementary Materials and Methods) did not show any involvement in splicing functional changes. Given our results and the possible uncertainty of this kind of prediction, further experimental validation is warranted. Unfortunately, no data are available on the different activities or expression levels of these two isoforms. Predictive functional analysis of the three significant SNPs in our study with PupaSuite software (http://pupasuite.bioinfo.cipf.es/) showed that rs1014666 and rs2508784 were contained in highly conserved regions of the genome. Less expected was the correlation between *XPA* SNPs and ionizing radiation-induced H2AX phosphorylation at 1 h.

The XPA protein is one of the six core components of the human NER pathway [26], which is a complex multi-step process that requires the participation of at least 30 proteins [27,28] and involves damage recognition, unwinding of the DNA helix near the lesion, dual incisions, removal of the stretch of DNA containing the lesion, re-synthesis of DNA to replace the damaged stretch, and

Table 5
Association between *MRE11A* gene haplotypes and % of γH2AX dephosphorylation at 3 h.

Haplotype ID	rs584531	rs581002	rs13447720	rs13447717	rs1014666	rs499952	rs16920467	rs680695	Frequency (*n*)	Frequency (%)
#10	G	G	A	A	A	C	A	A	67	28.4
#1	A	A	A	A	G	A	A	G	54	22.9
#7	A	G	G	A	A	C	A	A	49	20.8
#6	A	G	A	G	G	A	A	A	32	13.5
#5	A	G	A	A	G	C	T	G	13	5.5
#3	A	G	A	A	G	A	A	A	9	3.8
#4	A	G	A	A	G	A	A	G	5	2.1
#8	A	G	G	A	A	C	A	A	2	0.9
#9	A	G	G	A	A	C	A	A	2	0.9
#2	A	A	A	A	G	C	A	A	1	0.4
#11	G	G	A	A	A	C	T	G	1	0.4
#12	G	G	A	A	G	C	T	G	1	0.4

Haplotype ID	Number of subjects			% of γH2AX dephosphorylation at 3 h mean + SD			*p*-Value[a]
	0 copies	1 copy	2 copies	0 copies	1 copy	2 copies	
#10	64	41	13	19.64 ± 10.27	19.94 ± 12.03	11.11 ± 6.75	0.025
#1	71	40	7	18.08 ± 10.60	18.89 ± 11.05	25.63 ± 11.86	0.281
#7	74	39	5	19.34 ± 11.20	18.53 ± 10.59	13.03 ± 7.62	0.298
#6	89	26	3	17.71 ± 10.95	21.17 ± 9.88	30.68 ± 9.48	0.032
#5	105	13	0	18.19 ± 10.95	23.74 ± 9.17		0.055
#3	109	9	0	18.68 ± 10.93	20.37 ± 10.72		0.609
#4, #8, #9, #2, #11, #12	106	12	0	19.64 ± 11.03	11.45 ± 5.59		0.010

[a] *p*-Values from the Kruskal–Wallis or Wilcoxon Rank Sum test as appropriate.

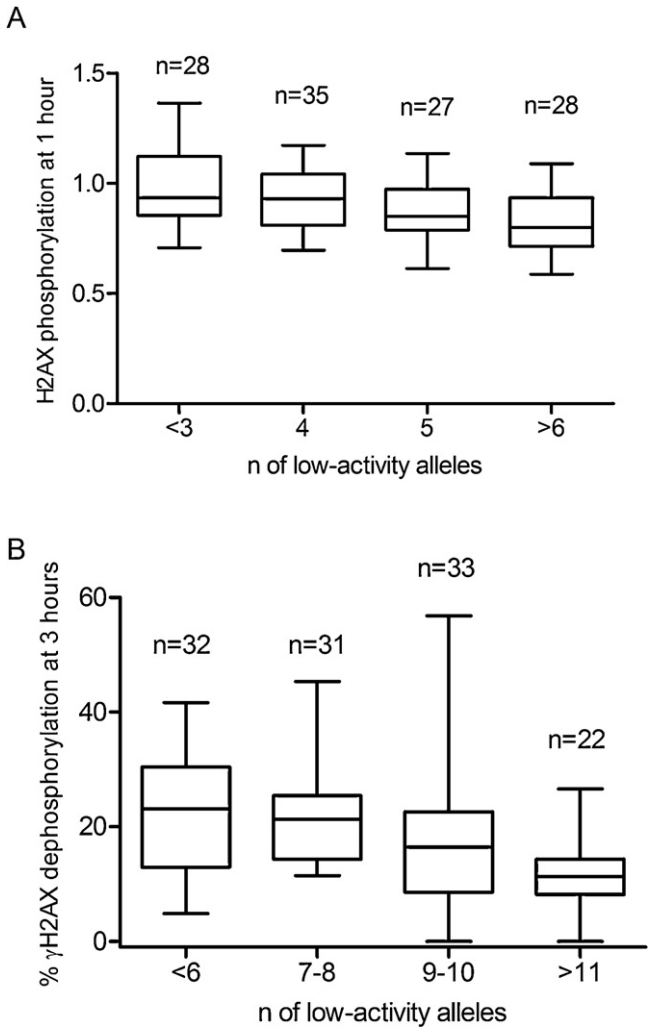

Fig. 1. Low-activity DSBR allele score. Relationship between the DSBR capacity (A: H2AX phosphorylation at 1 h; B: % of γH2AX dephosphorylation at 3 h) and the sum of low-activity alleles in DNA repair genes identified in Tables 2 and 3. The sum of low-activity alleles was computed for each subject by adding the number of alleles that have a putative effect on DSBR capacity (as per Tables 2 and 3). An increase in the total number of low-activity alleles was associated with (a) decreased DSB signaling capacity, as calculated from H2AX phosphorylation at 1 h (p-trend < 0.0001) and (b) decrease γH2AX dephosphorylation (p-trend < 0.0001). Data are presented as means, with standard errors represented by vertical bars.

finally ligation. It is believed that the XPA protein is involved in DNA damage recognition and also in the recruitment of other NER processes to the site of DNA damage to form dual incision complexes through protein–protein interactions [29,30]. Although the NER pathway is not known to be involved in the primary response to IR, genetic polymorphisms in XPF/ERCC1, XPG/ERCC5 and XPA did significantly influence the response to radiotherapy in patients with stages I and II head and neck cancer [31]. In addition, γ-irradiated cells with suppressed *XPA* gene expression exhibited a phenotype of elevated cell cycle progression and higher incidence of micronuclei, as well as a higher frequency of chromosome translocations, indicating the involvement of XPA in the regulation of DSBR [32]. These findings could suggest a role for the NER pathway in the repair of at least one type of IR-induced DNA damage.

Inter-strand crosslinks (ICLs) covalently link complementary strands of duplex DNA, and constitute a unique class of DNA damage that strongly inhibits DNA replication and transcription. ICLs are highly cytotoxic [33] and, interestingly, they represent a recently identified type of γ-ray damage [34]. XPA protein-deficient cells are ICL-removal defective, and a recent study indicated that in human cells containing ICLs, DSBs (as reflected by γH2AX) required XPF/ERCC1 for repair [35]. Equally intriguing, XPA protein-deficient cells had significantly higher γH2AX levels than normal control cells following ICL-inducing treatments. These higher γH2AX levels might be due to defective NER pathway-dependent removal of a large fraction of monoadducts and ICLs in these cells. If such is the case, the *XPA* gene SNP identified in this study, which correlated to decreased H2AX phosphorylation at 1 h, should confer improved ICL removal activity to the XPA protein. However, a concern related to time necessary for γH2AX formation as a consequence of ICL remains, and could weaken this interpretation.

In the present work, we found a correlation between only one *XPA* gene SNP/haplotype and H2AX phosphorylation at 1 h following IR, but in a previous report γH2AX was only barely detectable at 1.5 and 3 h after ICL-inducing treatments (HMT and UVA), and increased monotonically at later time points [35]. The slow kinetics of γH2AX formation contrast with the almost immediate appearance of γH2AX following ionizing radiation and is more consistent with the signaling of a secondary DSB generated as an intermediate response to ICL.

Alternatively, a direct link between XPA protein expression and/or activity and the kinases responsible for H2AX phosphorylation (ATR, ATM) might also explain our results. Evidence has been presented that the cellular function of XPA could be modulated by ATR, the primary transducer in the repair and replication of UV-induced DNA damage, which is also slowly activated following IR, Indeed, colocalization of XPA with ATR has been observed, at least in response to UV radiation [36].

Levels of phosphorylation of the ATM protein at Ser-1981 in response to cisplatin were found to be attenuated in XPA cells in a previous report [37]. This suggests the interesting possibility that the recruitment of the ATM protein to genomic DNA can also be mediated by components of the NER pathway, in addition to the well-known role of the MRN complex in recruiting ATM to DSB sites [20,38–41]. This view is intriguing in light of our present data, but remains to be fully demonstrated.

Finally, several research groups have identified *XPA* gene SNPs associated with cancer risk [42–44], but none of them found an association with rs3176683. As this SNP is neither in LD with any other *XPA* gene SNP associated with cancer, nor a non-synonymous SNP, further functional analyses are needed to confirm our results.

5. Conclusion

In conclusion, our study revealed that in addition to SNPs of genes that are well-established players in DSBR, non-DSBR genes such as the *XPA* gene, which has previously had only poorly recognized roles in DSBR, can in fact influence DSBR in healthy subjects. This suggests that successful DSBR requires both DSBR and non-DSBR mechanisms.

Funding

This work was supported by grants from the Associazione Italiana per la Ricerca sul Cancro (Italy; G.M., C.G.), the Progetto Integrato Oncologia, Regione Toscana – Ministero della Salute "Identification of population risk profiles as an approach to cancer prevention" and the Environmental Cancer Risk Nutrition and Individual Susceptibility Project (G.M.), a network of excellence operating within the European Union Sixth Framework Program, Priority 5: 'Food Quality and Safety' (Contract No. 513943). Partial funding for this project has also been received from the Compagnia di San Paolo (Turin, Italy; G.M.) and by the Progetto Ricerca Sanitaria Finalizzata Regione Piemonte (C.G., G.M.).

Conflict of interest statement

The authors declare that they have no conflict of interest.

Appendix A. Supplementary data

Supplementary data associated with this article can be found, in the online version, at doi:10.1016/j.dnarep.2011.08.003.

References

[1] E. Friedberg, G.C. Walker, W. Siede, DNA Repair and Mutagenesis, ASM Press, Washington, DC, 2006.
[2] M.F. Rajewsky, J. Engelbergs, J. Thomale, T. Schweer, Relevance of DNA repair to carcinogenesis and cancer therapy, Recent Results Cancer Res. 154 (1998) 127–146.
[3] M. Berwick, P. Vineis, Markers of DNA repair and susceptibility to cancer in humans: an epidemiologic review, J. Natl. Cancer Inst. 92 (2000) 874–897.
[4] E.L. Goode, C.M. Ulrich, J.D. Potter, Polymorphisms in DNA repair genes and associations with cancer risk, Cancer Epidemiol. Biomarkers Prev. 11 (2002) 1513–1530.
[5] P. Vineis, M. Manuguerra, F.K. Kavvoura, S. Guarrera, A. Allione, F. Rosa, A. Di Gregorio, S. Polidoro, F. Saletta, J.P. Ioannidis, G. Matullo, A field synopsis on low-penetrance variants in DNA repair genes and cancer susceptibility, J. Natl. Cancer Inst. 101 (2009) 24–36.
[6] K. Iijima, M. Ohara, R. Seki, H. Tauchi, Dancing on damaged chromatin: functions of ATM and the RAD50/MRE11/NBS1 complex in cellular responses to DNA damage, J. Radiat. Res. (Tokyo) 49 (2008) 451–464.
[7] M.F. Lavin, ATM and the Mre11 complex combine to recognize and signal DNA double-strand breaks, Oncogene 26 (2007) 7749–7758.
[8] S.P. Jackson, J. Bartek, The DNA-damage response in human biology and disease, Nature 461 (2009) 1071–1078.
[9] Y. Zhang, L.H. Rohde, H. Wu, Involvement of nucleotide excision and mismatch repair mechanisms in double strand break repair, Curr. Genomics 10 (2009) 250–258.
[10] R.D. Wood, M. Mitchell, J. Sgouros, T. Lindahl, Human DNA repair genes, Science 291 (2001) 1284–1289.
[11] R.D. Wood, M. Mitchell, T. Lindahl, Human DNA repair genes, Mutat. Res. 577 (2005) 275–283.
[12] S.H. MacPhail, J.P. Banath, Y. Yu, E. Chu, P.L. Olive, Cell cycle-dependent expression of phosphorylated histone H2AX: reduced expression in unirradiated but not X-irradiated G1-phase cells, Radiat. Res. 159 (2003) 759–767.
[13] G. Coutinho, J. Xie, L. Du, A. Brusco, A.R. Krainer, R.A. Gatti, Functional significance of a deep intronic mutation in the ATM gene and evidence for an alternative exon 28a, Hum. Mutat. 25 (2005) 118–124.
[14] P. Porcedda, V. Turinetto, A. Brusco, S. Cavalieri, E. Lantelme, L. Orlando, U. Ricardi, A. Amoroso, D. Gregori, C. Giachino, A rapid flow cytometry test based on histone H2AX phosphorylation for the sensitive and specific diagnosis of ataxia telangiectasia, Cytometry A 73 (2008) 508–516.
[15] J.C. Barrett, B. Fry, J. Maller, M.J. Daly, Haploview: analysis and visualization of LD and haplotype maps, Bioinformatics 21 (2005) 263–265.
[16] M. Stephens, N.J. Smith, P. Donnelly, A new statistical method for haplotype reconstruction from population data, Am. J. Hum. Genet. 68 (2001) 978– 989.
[17] M. Stephens, P. Donnelly, A comparison of bayesian methods for haplotype reconstruction from population genotype data, Am. J. Hum. Genet. 73 (2003) 1162–1169.
[18] A.M. Taylor, A. Groom, P.J. Byrd, Ataxia-telangiectasia-like disorder (ATLD)-its clinical presentation and molecular basis, DNA Repair (Amst) 3 (2004) 1219–1225.
[19] R.S. Williams, J.S. Williams, J.A. Tainer, Mre11–Rad50–Nbs1 is a keystone complex connecting DNA repair machinery, double-strand break signaling, and the chromatin template, Biochem. Cell Biol. 85 (2007) 509–520.
[20] T. Uziel, Y. Lerenthal, L. Moyal, Y. Andegeko, L. Mittelman, Y. Shiloh, Requirement of the MRN complex for ATM activation by DNA damage, Embo J. 22 (2003) 5612–5621.
[21] C.J. Bakkenist, M.B. Kastan, DNA damage activates ATM through intermolecular autophosphorylation and dimer dissociation, Nature 421 (2003) 499– 506.
[22] C.T. Carson, R.A. Schwartz, T.H. Stracker, C.E. Lilley, D.V. Lee, M.D. Weitzman, The Mre11 complex is required for ATM activation and the G2/M checkpoint, Embo J. 22 (2003) 6610–6620.
[23] A. Choudhury, F. Elliott, M.M. Iles, M. Churchman, R.G. Bristow, D.T. Bishop, A.E. Kiltie, Analysis of variants in DNA damage signalling genes in bladder cancer, BMC Med. Genet. 9 (2008) 69.
[24] M.A. Loizidou, T. Michael, S.L. Neuhausen, R.F. Newbold, Y. Marcou, E. Kakouri, M. Daniel, P. Papadopoulos, S. Malas, A. Hadjisavvas, K. Kyriacou, DNA-repair genetic polymorphisms and risk of breast cancer in Cyprus, Breast Cancer Res. Treat. 115 (2009) 623–627.
[25] S. Rollinson, H. Kesby, G.J. Morgan, Haplotypic variation in MRE11, RAD50 and NBS1 and risk of non-Hodgkin's lymphoma, Leuk. Lymphoma 47 (2006) 2567–2583.
[26] J.H. Hoeijmakers, Genome maintenance mechanisms for preventing cancer, Nature 411 (2001) 366–374.
[27] J. de Boer, J.H. Hoeijmakers, Nucleotide excision repair and human syndromes, Carcinogenesis 21 (2000) 453–460.
[28] D.P. Batty, R.D. Wood, Damage recognition in nucleotide excision repair of DNA, Gene 241 (2000) 193–204.
[29] U. Camenisch, H. Nageli, XPA gene, its product and biological roles, Adv. Exp. Med. Biol. 637 (2008) 28–38.
[30] D.L. Croteau, Y. Peng, B. Van Houten, DNA repair gets physical: mapping an XPA-binding site on ERCC1, DNA Repair (Amst) 7 (2008) 819–826.
[31] J. Carles, M. Monzo, M. Amat, S. Jansa, R. Artells, A. Navarro, P. Foro, F. Alameda, A. Gayete, B. Gel, M. Miguel, J. Albanell, X. Fabregat, Single-nucleotide polymorphisms in base excision repair, nucleotide excision repair, and double strand break genes as markers for response to radiotherapy in patients with Stage I to II head-and-neck cancer, Int. J. Radiat. Oncol. Biol. Phys. 66 (2006) 1022–1030.
[32] Y. Zhang, L.H. Rohde, K. Emami, D. Hammond, R. Casey, S.K. Mehta, A.S. Jeevarajan, D.L. Pierson, H. Wu, Suppressed expression of non-DSB repair genes inhibits gamma-radiation-induced cytogenetic repair and cell cycle arrest, DNA Repair (Amst) 7 (2008) 1835–1845.
[33] M.L. Dronkert, R. Kanaar, Repair of DNA interstrand cross-links, Mutat. Res. 486 (2001) 217–247.
[34] S. Cecchini, S. Girouard, M.A. Huels, L. Sanche, D.J. Hunting, Interstrand cross-links: a new type of gamma-ray damage in bromodeoxyuridine-substituted DNA, Biochemistry 44 (2005) 1932–1940.
[35] S. Mogi, D.H. Oh, gamma-H2AX formation in response to interstrand crosslinks requires XPF in human cells, DNA Repair (Amst) 5 (2006) 731–740.
[36] X. Wu, S.M. Shell, Z. Yang, Y. Zou, Phosphorylation of nucleotide excision repair factor xeroderma pigmentosum group A by ataxia telangiectasia mutated and Rad3-related-dependent checkpoint pathway promotes cell survival in response to UV irradiation, Cancer Res. 66 (2006) 2997–3005.
[37] S.L. Colton, X.S. Xu, Y.A. Wang, G. Wang, The involvement of ataxia-telangiectasia mutated protein activation in nucleotide excision repair-facilitated cell survival with cisplatin treatment, J. Biol. Chem. 281 (2006) 27117.
[38] J.H. Lee, T.T. Paull, Direct activation of the ATM protein kinase by the Mre11/Rad50/Nbs1 complex, Science 304 (2004) 93–96.
[39] J.H. Lee, T.T. Paull, ATM activation by DNA double-strand breaks through the Mre11–Rad50–Nbs1 complex, Science 308 (2005) 551–554.
[40] Z. You, C. Chahwan, J. Bailis, T. Hunter, P. Russell, ATM activation and its recruitment to damaged DNA require binding to the C terminus of Nbs1, Mol. Cell. Biol. 25 (2005) 5363–5379.
[41] T.T. Paull, J.H. Lee, The Mre11/Rad50/Nbs1 complex and its role as a DNA double-strand break sensor for ATM, Cell Cycle 4 (2005) 737–740.
[42] D. Palli, S. Polidoro, M. D'Errico, C. Saieva, S. Guarrera, A.S. Calcagnile, F. Sera, A. Allione, S. Gemma, I. Zanna, A. Filomena, E. Testai, S. Caini, R. Moretti, M.J. Gomez-Miguel, G. Nesi, I. Luzzi, L. Ottini, G. Masala, G. Matullo, E. Dogliotti, Polymorphic DNA repair and metabolic genes: a multigenic study on gastric cancer, Mutagenesis 25 (2010) 569–575.
[43] B. Qian, H. Zhang, L. Zhang, X. Zhou, H. Yu, K. Chen, Association of genetic polymorphisms in DNA repair pathway genes with non-small cell lung cancer risk, Lung Cancer 73 (2011) 138–146.
[44] C. Kiyohara, K. Yoshimasu, Genetic polymorphisms in the nucleotide excision repair pathway and lung cancer risk: a meta-analysis, Int. J. Med. Sci. 4 (2007) 59–71.